Loss of the BH3-only protein Bmf impairs B cell homeostasis and accelerates γ irradiation–induced thymic lymphoma development

Verena Labi,[1] Miriam Erlacher,[1] Stephan Kiessling,[1] Claudia Manzl,[1] Anna Frenzel,[1] Lorraine O'Reilly,[2] Andreas Strasser,[2] and Andreas Villunger[1]

[1]Division of Developmental Immunology, Biocenter, Innsbruck Medical University, 6020 Innsbruck, Austria
[2]The Walter and Eliza Hall Institute of Medical Research, Melbourne, Victoria 3050, Australia

Members of the Bcl-2 protein family play crucial roles in the maintenance of tissue homeostasis by regulating apoptosis in response to developmental cues or exogenous stress. Proapoptotic BH3-only members of the Bcl-2 family are essential for initiation of cell death, and they function by activating the proapoptotic Bcl-2 family members Bax and/or Bak, either directly or indirectly through binding to prosurvival Bcl-2 family members. Bax and Bak then elicit the downstream events in apoptosis signaling. Mammals have at least eight BH3-only proteins and they are activated in a stimulus-specific, as well as a cell type–specific, manner. We have generated mice lacking the BH3-only protein Bcl-2–modifying factor (Bmf) to investigate its role in cell death signaling. Our studies reveal that Bmf is dispensable for embryonic development and certain forms of stress-induced apoptosis, including loss of cell attachment (anoikis) or UV irradiation. Remarkably, loss of Bmf protected lymphocytes against apoptosis induced by glucocorticoids or histone deacetylase inhibition. Moreover, *bmf*$^{-/-}$ mice develop a B cell–restricted lymphadenopathy caused by the abnormal resistance of these cells to a range of apoptotic stimuli. Finally, Bmf-deficiency accelerated the development of γ irradiation–induced thymic lymphomas. Our results demonstrate that Bmf plays a critical role in apoptosis signaling and can function as a tumor suppressor.

CORRESPONDENCE
Andreas Villunger:
andreas.villunger@i-med.ac.at

Abbreviations used: BCR, B cell receptor; BH, Bcl-2 homology; Bmf, Bcl-2–modifying factor; CBHA, m-carboxycinnamic acid bis-hydroxamide; DLC, dynein light chain; DN, double-negative; DP, double-positive; ES, embryonic stem; HDAC, histone deacetylase; MEF, mouse embryonic fibroblast; PI, propidium iodide; SAHA, suberoylanilide hydroxamic acid; SP, single-positive; TNF-R, tumor necrosis factor receptor.

Deletion of no longer needed or potentially harmful cells by apoptosis acts as an essential barrier against a variety of diseases, including autoimmunity and cancer (1, 2). Apoptosis can be triggered either via the so-called extrinsic pathway by ligation of "death receptors," which are members of the tumor necrosis factor receptor (TNF-R) family, with an intracellular "death domain" (e.g., Fas/APO-1/CD95, TNF-R1, DR4, and DR5) or through the "mitochondrial" (also called "intrinsic" or "Bcl-2–regulated") pathway, which is induced by developmental cues, growth factor deprivation, or a range of cytotoxic stimuli and regulated by the interactions between pro- and antiapoptotic members of the Bcl-2 protein family (2). Members of the Bcl-2 family are characterized by structural motifs, called Bcl-2 homology (BH) domains. The prosurvival family members Bcl-2, Bcl-x_L, Bcl-w, A1/Bfl-1, and Mcl-1 contain up to four BH domains (BH1–4), whereas proapoptotic Bax, Bak, and Bok (Mtd) possess three BH domains (BH1, BH2, and BH3), and the BH3-only proteins possess only the BH3 domain (1).

The BH3-only proteins Bik/Blk/Nbk, Bid, Bad, Hrk/DP5, Noxa/Apr, Bcl-2–modifying factor (Bmf), Puma/Bbc3, and Bim/Bod can all induce cell death when overexpressed in cells in tissue culture (2). Induction of apoptosis by BH3-only proteins requires Bax or Bak (3, 4), but how these proteins induce cell death is still not entirely clear. According to one model, certain BH3-only proteins (Bim, caspase-activated tBid, and perhaps Puma) activate Bax/Bak by direct binding, whereas the other BH3-only

A. Strasser and A. Villunger contributed equally to this paper.
M. Erlacher's present address is Dept. of Pediatrics and Adolescent Medicine, University Hospital of Freiburg, 79104 Freiburg, Germany.
The online version of this article contains supplemental material.

proteins promote apoptosis by binding and neutralization of the prosurvival Bcl-2 family members (5). The competing model proposes that BH3-only proteins activate apoptosis by binding only to the prosurvival Bcl-2–like proteins, thereby liberating Bax and Bak (6). BH3-only proteins are thought to differ in their apoptotic potency because they differ in their ability to bind to the prosurvival Bcl-2 family members. For example, Bim and Puma bind all Bcl-2–like prosurvival proteins with high affinity, whereas Noxa binds only Mcl-1 and A1 and, conversely, Bmf and Bad bind only to Bcl-2, Bcl-x_L, and Bcl-w (7, 8).

The roles of BH3-only proteins in normal physiology and stress-induced apoptosis have been addressed by gene targeting in mice. Deletion of any single BH3-only gene does not markedly perturb embryonic development, with the exception of Bim loss, which causes the death of >40% of embryos before embryonic day 10 (unpublished data) (9). These and other observations indicate an extensive degree of functional redundancy between BH3-only proteins, and this was formally demonstrated by the finding that $bim^{-/-}bik^{-/-}$ males have severe defects in spermatogenesis, whereas males lacking only Bim or Bik are normally fertile (10). Interesting cell type– and death stimulus–specific defects have been observed in some knockout mouse strains lacking individual BH3-only proteins (1). For example, loss of Bid renders hepatocytes resistant to anti-Fas antibody– or FasL-induced apoptosis, whereas lymphoid cells remain normally sensitive, demonstrating that the Bid-mediated connection between the extrinsic and the intrinsic apoptotic pathway is only critical in certain cell types (11, 12). Lymphocytes and certain other cell types from mice lacking *puma* are refractory to p53-induced apoptosis triggered by DNA damage. Interestingly, some p53-independent pathways to apoptosis, such as those triggered by cytokine deprivation or treatment with glucocorticoids or phorbol esters, also rely on Puma (13–15). Loss of Bim protects lymphoid cells against cytokine deprivation, deregulated Ca^{2+}-flux, and also glucocorticoids, indicating some functional overlap between Bim and Puma (9, 16). In addition, Bim deficiency interferes with the deletion of autoreactive T and B cells (17–19) and impairs the death of antigen-activated T cells during shutdown of an acute immune response (20, 21).

Little is known about the physiological role of Bmf, which shares certain features with Bim. For example, both proteins were reported to interact with dynein light chain (DLC) molecules, small components of cytoskeleton-associated motor complexes such as the microtubule-based dynein motor complex containing DLC1, or the actin-based myosin V motor complex, containing DLC2. DLC1 was reported to sequester Bim to the microtubular dynein motor complex, whereas DLC2 targets Bmf to the actin-bound myosin V motor complex (22, 23). In response to certain apoptotic stimuli, Bim and/or Bmf can be released from the cytoskeleton, translocate to mitochondria, and neutralize Bcl-2 prosurvival molecules to trigger Bax/Bak activation and caspase-mediated cell killing. UV irradiation, for example, causes release of both proteins, whereas Bmf seems to be specifically activated in response to loss of cell attachment, a death stimulus that is

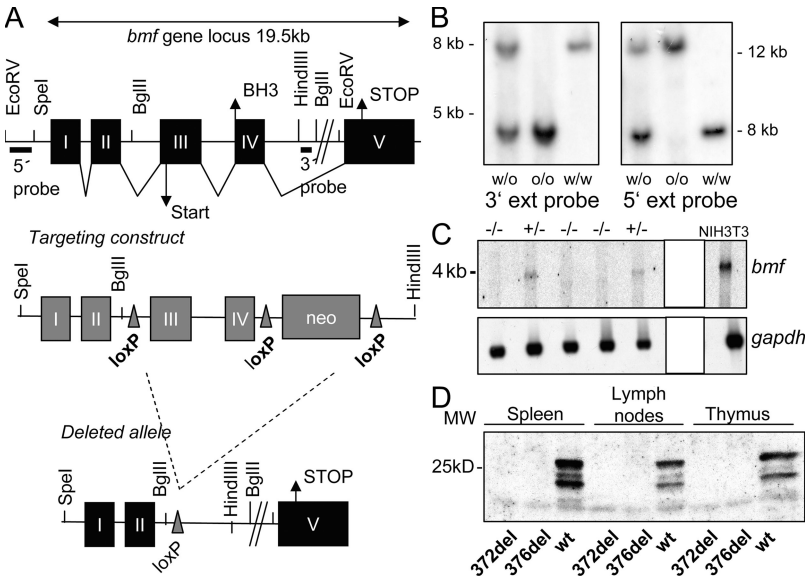

Figure 1. Generation of $bmf^{-/-}$ mice by homologous recombination. (A) Schematic representation of the *bmf* gene locus on mouse chromosome 2. Exons 3 and 4, as well as the neomycin selection marker, were flanked by *loxP* elements in the targeting construct. Exons 3 and 4, as well as the neomycin selection marker cassette, were removed in vivo by cre-mediated deletion using *Ubi-cre* deleter mice (dashed lines). The location of the 5′ and 3′ probes used for Southern blot analysis are indicated as black bars. (B) Southern blot analysis of liver-derived DNA from WT, $bmf^{+/-}$, and $bmf^{-/-}$ mice using 5′ and 3′ external probes. (C) Analysis of *bmf* mRNA expression in MEFs by Northern blot analysis. (D) Bmf protein expression analysis by Western blotting in extracts from thymus, spleen, or lymph nodes derived from WT and both strains of Bmf-deficient mice, which had been generated from independent ES cell clones.

called anoikis (22, 23). In addition, studies with certain tumor-derived cell lines have indicated that Bmf is critical for killing of these cells induced by treatment with histone deacetylase inhibitors (HDACi) (24). Interestingly, the *bim* and *bmf* genes are located near each other on mouse chromosome 2 and on syntenic regions on human chromosome 2 and 15, respectively. This indicates that these genes may have arisen from a common ancestral BH3-only gene, although their homology today is restricted to the BH3 domain and DLC-binding motif. Importantly, human chromosome 15q14, the region where the Bmf gene resides, was reported to harbor a so far unidentified tumor suppressor that is frequently lost during the very late stages in breast and lung cancer development (25, 26).

To investigate the role of Bmf in normal development and physiology, we have generated mice lacking *bmf*. The analysis of these animals revealed so far unidentified roles for Bmf in lymphocyte apoptosis, B cell homeostasis, and suppression of γ irradiation–induced thymic lymphoma development.

RESULTS

Generation of Bmf-deficient mice

Our gene targeting approach was designed to remove exons 3 and 4 of *bmf*, which contain the start codon and the BH3-domain, respectively (Fig. 1 A). Correct targeting of the *bmf* gene locus was confirmed by Southern blot analysis of genomic DNA from embryonic stem (ES) cells (not depicted) and liver of knockout mice, using 5′and 3′external probes (Fig. 1, A and B). Absence of *bmf* mRNA was verified by Northern blot analysis of polyA$^+$ mRNA from mouse embryonic fibroblasts (MEFs; Fig. 1 C), and the absence of the protein was confirmed in lysates from spleen, lymph nodes, and thymus of animals from two independently derived knockout lines using a Bmf-specific monoclonal antibody (Fig. 1 D). Consistent with a previous study from human cells (27), these tissues express two or three distinct Bmf isoforms; importantly, all Bmf isoforms were deleted by our gene-targeting approach.

Analysis of heterozygous intercrosses of *bmf*$^{+/-}$ mice revealed that Bmf-deficient animals were born at the expected Mendelian frequency, indicating that Bmf is dispensable for embryonic development. Animals lacking Bmf did not display any obvious phenotypic abnormalities, gender bias, or impaired fertility. Finally, histological examination of heart, lung, liver, kidney, and testis derived from 6–8-wk-old animals did not reveal any gross abnormalities (unpublished data).

Bmf is critical for glucocorticoid- and HDAC inhibitor–induced thymocyte apoptosis

Bmf proteins are expressed at significant levels in hemopoietic tissues (Fig. 1 D), but it was not clear which cell types do express Bmf. Therefore, immature CD4$^+$8$^+$ thymocytes, mature T and B cells from the spleen, B cell precursors from bone marrow, and T and B cell blasts generated by stimulation of splenocytes with ConA or LPS, respectively, were isolated by FACS sorting and subjected to Western blotting using Bmf-specific monoclonal antibodies. Our analysis revealed that Bmf expression was highest in immature CD4$^+$8$^+$ (DP) thymocytes, but comparatively lower in mature resting T cells or mitogen-stimulated T cell blasts (Fig. 2 A). Bmf expression was found throughout B cell development with one notable exception: pro–B cells (Fig. 2 A). Interestingly, expression of Bim was also detected from the pre–B cell stage onward and appeared strongest in CD4$^+$8$^+$ thymocytes and CD8$^+$ T cells (Fig. 2 A). Loss of Bmf did not cause compensatory

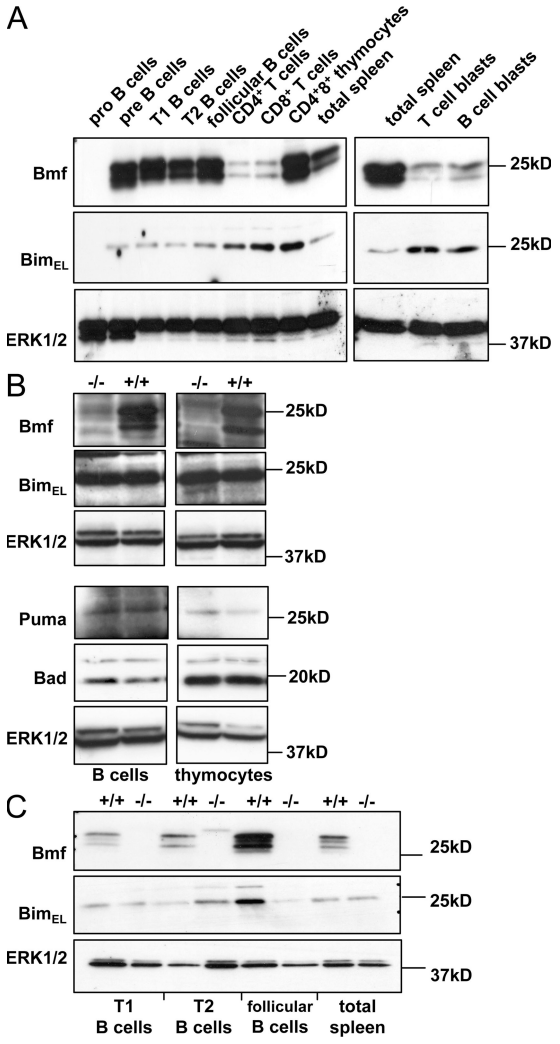

Figure 2. Expression analysis of Bmf and Bim in different leukocyte subsets. (A) Cells of the indicated differentiation stages were isolated from WT mice by cell surface marker staining and FACS sorting. Cells were lysed, and proteins were size fractioned by SDS-PAGE and transferred onto nitrocellulose membranes. Protein expression was evaluated using monoclonal antibodies recognizing mouse Bmf, Bim, or ERK (loading control). Membranes were stripped before subsequent reprobing with anti-Bim– and -ERK–specific antibodies, respectively. (B) Total thymocytes and CD19$^+$ B cells from WT and *bmf*$^{-/-}$ mice were analyzed for expression of Bim, Bad, and Puma. Reprobing with an anti-ERK–specific antibody served as loading control. (C) B cell subsets of the indicated differentiation stages were isolated from WT or Bmf-deficient mice by cell surface marker staining and FACS sorting and processed as in A.

up-regulation of other BH3-only proteins such as Bim, Bad, or Puma (Fig. 2 B).

Next, we compared the overall leukocyte subset composition of primary and secondary lymphoid organs between 6–8-wk-old WT and *bmf*$^{-/-}$ animals. Bim-deficient animals show a well-defined phenotype in the hemopoietic system (9, 16) and were included in our analysis as a reference. Total thymic cellularity, as well as the percentages and overall numbers of all four major thymocyte subsets (CD4$^-$8$^-$ double-negative (DN), CD4$^+$8$^+$ double-positive (DP), and CD4$^+$8$^-$ and CD4$^-$8$^+$ single-positive (SP) cells were comparable between WT and Bmf-deficient animals (Table I). The percentages and numbers of cells expressing low or high levels of T cell receptor (TCR) β were also indistinguishable between mice of both genotypes (unpublished data). In contrast, Bim-deficient animals displayed the previously described abnormal thymic cell subset composition (9), which is characterized by reduced percentages and overall numbers of DP thymocytes and an accumulation of mature (TCRα/β$^+$) DN and SP thymocytes (Table I).

To investigate a possible role for Bmf in stress-induced apoptosis, thymocytes from WT and Bmf-deficient animals were put in culture without further treatment (spontaneous death) or exposed to the phorbol ester PMA, the calcium ionophore ionomycin, the DNA damage–inducing drug VP16, the glucocorticoid dexamethasone, the broad-spectrum kinase inhibitor staurosporin, the glycosylation inhibitor and ER stressor tunicamycin, or the histone-deacetylase inhibitors Trichostatin A, m-carboxycinnamic acid bis-hydroxamide (CBHA), or suberoylanilide hydroxamic acid (SAHA; also known as vorinostat). Responses to glucocorticoids and HDAC inhibitors were of particular interest because Bmf has previously been implicated in apoptosis induction of primary childhood leukemia cells by glucocorticoids (28), as well as esophageal squamous cell carcinoma lines by CBHA (24). Thymocytes from mice lacking Puma, which were previously shown to be resistant to spontaneous death, DNA damage, glucocorticoids and PMA (13), were included as controls in these assays. Bmf-deficient thymocytes were normally sensitive to most apoptotic stimuli tested, including spontaneous death (Fig. 3 A), but remarkably, they were abnormally resistant to VP16 (Fig. 3 B), dexamethasone (Fig. 3 C), and HDAC inhibition by SAHA (Fig. 3 D). Curiously, *bmf*$^{-/-}$ thymocytes were almost as sensitive as WT cells to HDAC inhibition by CBHA or Trichostatin A (Fig. S1, A and B, available at http://www.jem.org/cgi/content/full/jem.20071658/DC1). Consistent with the inhibition of apoptosis, activation of caspase-3 was delayed in *bmf*$^{-/-}$ thymocytes treated with dexamethasone (Fig. 3 E) or SAHA (Fig. 3 F). In line with its relatively low expression in mature CD4$^+$ and CD8$^+$ T cells, loss of Bmf had no effect on the response of these cells to any of the cytotoxic stimuli tested (unpublished data). Consistent with the observation that Bcl-2 overexpression does not protect lymphocytes against Fas-induced apoptosis (29), loss of Bmf had no effect on FasL-induced killing (unpublished data). In addition, assessment of the viability of thymocytes (mean viability WT 95.56% vs.

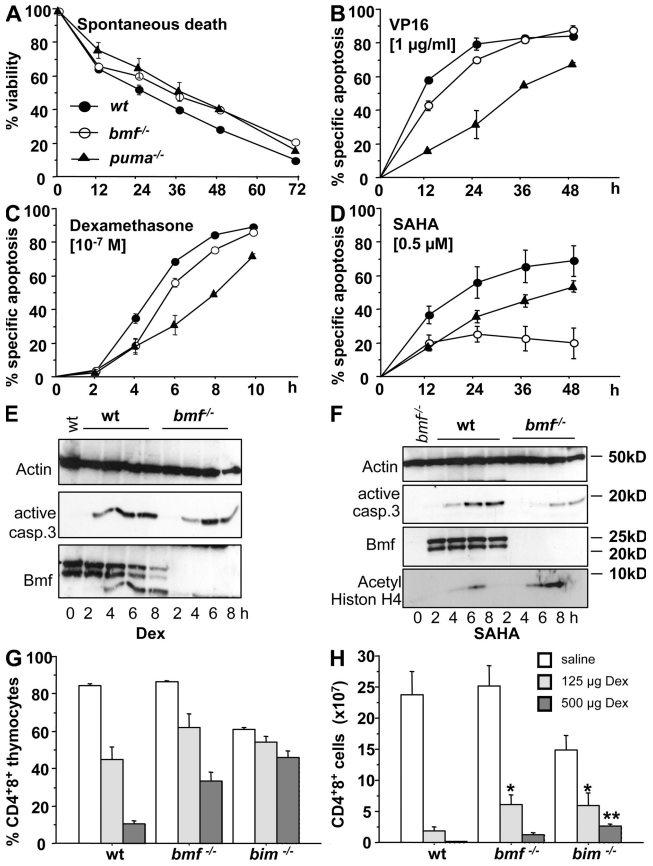

Figure 3. Bmf-deficient thymocytes are abnormally resistant to certain apoptotic stimuli. (A) Total thymocytes from mice of the indicated genotypes were put in culture without further treatment (spontaneous death; A) or exposed to the DNA-damaging drug VP16 (etoposide; B), dexamethasone (C), or the HDAC inhibitor SAHA (D). Cell death was monitored by Annexin V-FITC/PI staining and flow cytometric analysis at the indicated time points. The extent of apoptosis induced specifically by different stimuli was calculated by the following equation: (induced apoptosis − spontaneous cell death)/(100 − spontaneous cell death). Means ± the SEM from four independent experiments and $n = 5$ animals per genotype are shown. Significant differences in cell death induction were observed between WT and Bmf-deficient cells treated with VP16 ($P = 0.0096$), dexamethasone ($P = 0.0048$), or SAHA ($P = 0.0089$) using ANOVA analysis. Thymocytes from WT and Bmf-deficient mice were evaluated for caspase-3 activation in response to dexamethasone (E) or HDAC inhibition by SAHA (F) using an antibody specifically recognizing the proteolytically generated active p17 fragment of caspase-3. Filters were reprobed using antibodies specific for Bmf or β-actin (loading control). Reactivity of SAHA was confirmed using an antibody recognizing acetylated histone H4 (Lys12) that was showing highest reactivity after 6 h. 8–10-wk-old female mice of the indicated genotypes were injected with graded doses of dexamethasone, and the percentages (G) and number (H) of surviving CD4$^+$8$^+$ thymocytes were assessed 20 h later by cell counting of single-cell suspensions and flow cytometric analysis of CD4 and CD8 cell surface marker expression. Bars represent the mean ± the SEM of 8 WT, 8 *bmf*$^{-/-}$, and ≥3 *bim*$^{-/-}$ mice per treatment and ≥3 independent experiments. Using analysis of variance, significant differences (*) in the numbers of surviving thymocytes were observed between WT, *bmf*$^{-/-}$, and *bim*$^{-/-}$ mice using 125 µg dexamethasone/mouse ($P < 0.04$) and between WT and *bim*$^{-/-}$ mice using 500 µg dexamethasone ($P = 0.007$).

Table I. Composition of primary and secondary lymphatic organs of Bmf-deficient mice

Cell populations	WT	*bmf* $^{-/-}$	*bim* $^{-/-}$
Thymus			
Total cellularity (×10^7)	26.56 ± 2.28	29.07 ± 2.44	22.47 ± 3.29
$CD4^+$ cells	2.38 ± 0.19	1.94 ± 0.16	4.85 ± 0.81[a]
$CD8^+$ cells	0.93 ± 0.08	0.84 ± 0.09	1.6 ± 0.23[a]
$CD4^+8^+$ cells	22.28 ± 2.02	25.25 ± 2.17	13.84 ± 2.13[a]
$CD4^-8^-$ cells	0.98 ± 0.1	1.03 ± 0.11	2.15 ± 0.28[a]
Bone marrow			
Total cellularity (×10^6)	31.37 ± 2.4	40.19 ± 2.44[a]	34.7 ± 2.63
T cells	1.26 ± 0.15	1.45 ± 0.09	2.85 ± 0.31[a]
Myeloid cells	12.91 ± 1.41	15.12 ± 1.42	9.73 ± 0.75
Erythroid progenitors	12.13 ± 1.11	10.27 ± 0.82	6.78 ± 0.62[a]
B cells	8.87 ± 1.15	15.57 ± 1.28[a]	10.67 ± 0.93
Pro B cells	1.61 ± 0.23	1.78 ± 0.11	2.61 ± 0.37[a]
Pre B cells	4.66 ± 0.49	6.69 ± 0.52[a]	4.94 ± 0.62
T1 B cells	1.06 ± 0.19	1.86 ± 0.22[a]	1.32 ± 0.43
Mature B cells	1.73 ± 0.19	4.29 ± 0.48[a]	4.07 ± 0.99[a]
Spleen			
Total cellularity (×10^7)	16.19 ± 1.42	26.1 ± 2.13[b]	36.86 ± 3.32[a]
$CD4^+$ T cells	2.76 ± 0.25	2.84 ± 0.24	5.12 ± 0.42[a]
$CD8^+$ T cells	1.7 ± 0.3	2.01 ± 0.18	4.21 ± 0.41[a]
Myeloid cells	1.1 ± 0.21	1.3 ± 0.17	1.07 ± 0.12
Erythroid progenitors	1.67 ± 0.39	2.09 ± 0.36	3.59 ± 0.32[a]
B cells	9.56 ± 0.98	18.79 ± 0.15[b]	22.3 ± 2.13[b]
White blood cells			
Total cellularity (×10^6/ml)	8.76 ± 0.89	12.31 ± 0.91	22.4 ± 3.83[a]
$CD4^+$ T cells	1.22 ± 0.26	0.96 ± 0.14	2.02 ± 0.31
$CD8^+$ T cells	0.97 ± 0.2	0.84 ± 0.07	2.77 ± 0.38[a]
Myeloid cells	1.56 ± 0.3	1.12 ± 0.13	1.41 ± 0.22
B cells	5.71 ± 0.62	9.01 ± 0.79[a]	16.25 ± 2.86[a]
T1 B cells	0.51 ± 0.08	0.8 ± 0.1[a]	1.47 ± 0.31[a]
Inguinal lymph nodes			
Total cellularity (×10^6)	9.75 ± 1.05	17.81 ± 1.47[a]	21.25 ± 3.55[a]
$CD4^+$ T cells	3.98 ± 0.51	5.44 ± 0.48	7.86 ± 1.09[a]
$CD8^+$ T cells	2.67 ± 0.29	4.51 ± 0.42[a]	11.99 ± 1.41[a]
B cells	2.75 ± 0.58	7.7 ± 0.92[a]	5.47 ± 0.97[a]

Total numbers of hemopoietic cells from 6–8-wk-old animals were calculated by counting single-cell suspensions derived from the indicated organs and tissues that were subsequently analyzed by flow cytometry after staining for cell surface markers: total T cells (Thy-1^+), total myeloid cells (Mac-1^+), total nucleated erythroid progenitor cells (Ter119^+), total B cells (B220^+), pro–B cells (B220^+CD43^+IgM$^-$), pre–B cells (B220^+CD43^-IgM$^-$), T1 B cells (sIgM^{high}CD21^{low}), and mature B cells (sIgM^{low}IgD$^+$). Numbers represent the mean (± the SEM) of 6 WT, 9 *bmf*$^{-/-}$, and 5 *bim*$^{-/-}$ mice. Total cellularity of both inguinal lymph nodes and femora are presented.
[a]$P < 0.05$ compared to WT mice.
[b]$P < 0.0001$ compared to WT mice.

bmf$^{-/-}$ 95.96%; $n = 4$) or mature T cells (mean viability WT 91.89% vs. *bmf*$^{-/-}$ 91.63%; $n = 4$) directly after organ harvest, by Annexin V/propidium iodide (PI) staining and flow cytometric analysis, did not reveal any differences in the steady-state level of T cell apoptosis in spleens and thymi from WT and *bmf*$^{-/-}$ mice.

To examine the role of Bmf in apoptosis induction in vivo, we measured T cell depletion after injection of graded doses of dexamethasone and compared it to effects observed in *bim*$^{-/-}$ mice. Interestingly, the percentage (Fig. 3 G) and number of $CD4^+8^+$ thymocytes (Fig. 3 H) that were recovered in *bmf*$^{-/-}$ or *bim*$^{-/-}$ mice 20 h after dexamethasone injection were significantly larger than those found in WT animals (Fig. 3, G and H). The extent of protection provided by Bmf deficiency was comparable to that afforded by the absence of Bim (Fig. 3, G and H) or Puma (30), indicating that glucocorticoids activate at least three BH3-only proteins to trigger cell death in mouse thymocytes.

Collectively, our data demonstrate that Bmf is dispensable for normal T cell development, but contributes to thymocyte apoptosis induced by certain cytotoxic stimuli, including treatment with glucocorticoids or HDAC inhibitors.

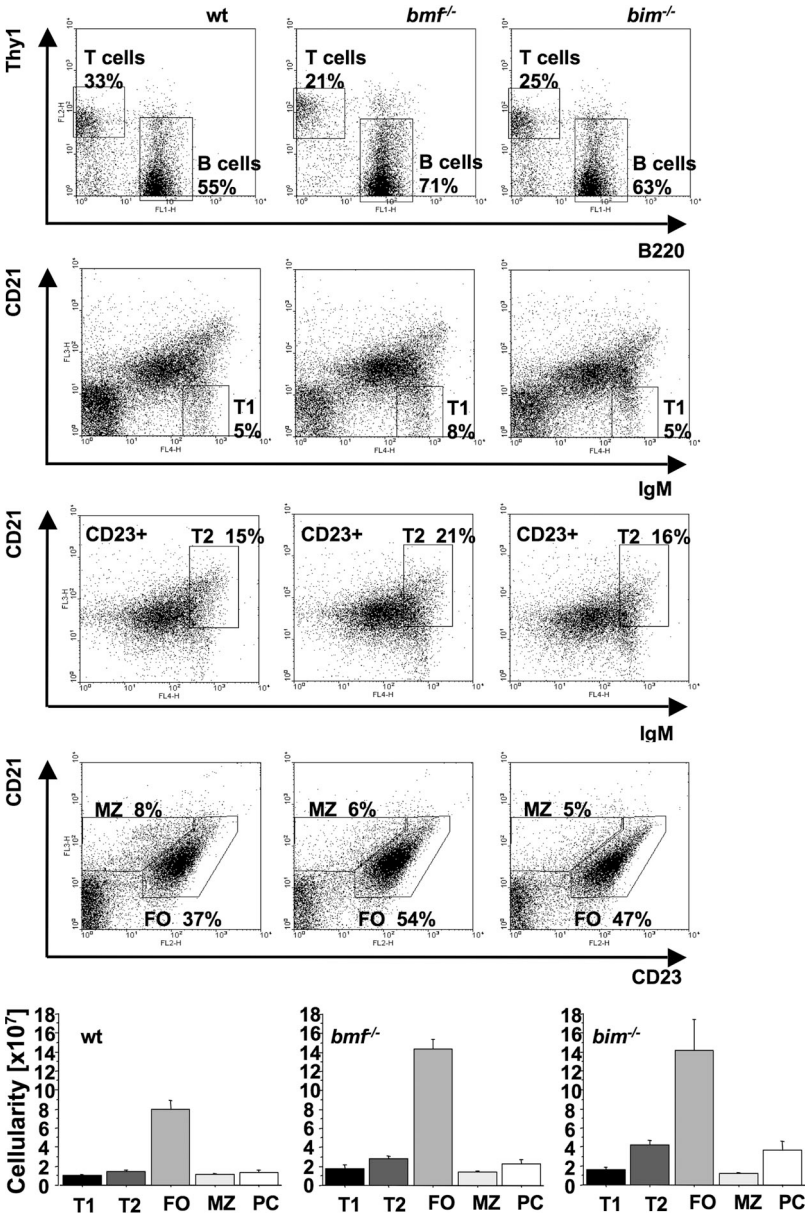

Figure 4. Loss of Bmf causes B cell hyperplasia. (A) Flow cytometric analysis of spleen-derived single-cell suspensions from WT, *bmf*$^{-/-}$, and *bim*$^{-/-}$ mice using antibodies against the T cell marker Thy1 and the B cell marker B220. Representative dot blots of spleen cells stained with different B cell maturation markers to identify different stages of B cell development: T1 transitional B cells (sIgM^{high}CD21^{+}); T2 transitional B cells (CD21^{+}CD23^{+}sIgM^{high}); mature follicular (FO) B cells (CD21^{+}CD23^{+}); marginal zone (MZ) B cells(CD21^{high}CD21^{-}); and plasma cells (PC; B220^{+}CD138^{+}). (bottom) Quantification of B cell subsets in the spleens derived from T, *bmf*$^{-/-}$, and *bim*$^{-/-}$ mice ($n = 4$) gathered in two independent experiments. Error bars represent the means ± the SEM. Using the unpaired Student's *t* test, significant differences between WT and *bmf*$^{-/-}$ or *bim*$^{-/-}$ mice were observed in T1 cells ($P < 0.039$), T2 cells ($P < 0.0019$), and FO cells ($P < 0.01$). The number of plasma cells was only significantly elevated in Bim-deficient mice (WT vs. *bim*$^{-/-}$; $P < 0.03$).

Bmf deficiency perturbs B cell homeostasis

Because Bmf protein expression was readily detectable at various stages of B cell development (Fig. 2), we quantified the numbers of pro–B (B220^{+}sIgM^{-}CD43^{+}), pre–B (B220^{+}sIgM^{-}CD43^{-}), and transitional (T1) B cells (sIgM^{high}CD21^{low}) in WT, *bmf*$^{-/-}$, and, as a control, *bim*$^{-/-}$ mice, which are known to have defects in developmentally programmed death of B lymphocytes (9, 19). A significant ($P < 0.05$) increase in pre–B cell numbers was evident in the bone marrow of Bmf-deficient mice, whereas pro–B cell numbers were normal (Table I). In contrast, pre–B cell numbers appeared normal in Bim-deficient animals (Table I), although Bim is expressed in this cell subset (Fig. 2). Shortly before immature B cells leave the bone marrow to continue their maturation in the spleen, the expression level of sIgM increases. T1 B cells were also abnormally elevated in *bmf*$^{-/-}$ mice (Table I), as were those of recirculating

mature IgM$^+$IgD^{high} B cells. The numbers of these two B lymphoid populations were also abnormally elevated in Bim-deficient mice, although only the increase in mature B cells was statistically significant (Table I). Collectively, these results indicate that not only Bim but also Bmf regulates the developmentally programmed death of B lymphoid cells.

Cell counting revealed a >50% increase in the overall splenic cellularity in Bmf-deficient mice and, as shown before (9), an ∼2–3-fold increase in *bim*$^{-/-}$ mice (Table I). Immunofluorescent staining with surface marker–specific antibodies and flow cytometric analysis revealed that the percentage of B220$^+$ B cells was significantly increased in *bmf*$^{-/-}$ mice, and that this increase was accompanied by a proportional decrease in the percentages of Thy1$^+$ T cells and Mac-1$^+$ myeloid cell (Fig. 4 A and not depicted). This finding was confirmed by staining splenocytes with antibodies recognizing the T cell markers CD4, CD8, or TCRβ (unpublished data). The overall numbers of mature CD4$^+$ and CD8$^+$ T cells in *bmf*$^{-/-}$ mice were, however, comparable to those observed in WT mice, and their abnormally low percentages were a consequence of the abnormal B cell expansion. In contrast, and as previously shown (9), excess numbers of both B and T lymphocytes were found in spleens of *bim*$^{-/-}$ mice (Table I).

Detailed analysis of different B cell maturation stages in the spleen (Fig. 4, B and E) revealed significantly elevated numbers of T1 transitional B cells in *bmf*$^{-/-}$ and *bim*$^{-/-}$ mice and a profound increase in T2 transitional B cells (CD21$^+$CD23$^+$sIgM^{high}), a subpopulation of sIgM$^+$sIgD$^+$ B cells that can give rise to mature sIgM^{low}sIgD$^+$ B cells in reconstitution experiments in *rag*$^{-/-}$ mice (31). Mature follicular B cells (CD21$^+$CD23$^+$) were also abnormally increased in both *bmf*$^{-/-}$ as well as *bim*$^{-/-}$ mice, but the numbers of marginal zone (MZ) B cells (CD21^{high}CD23$^-$), a subset of B cells that lines the border of the white pulp and is critical for responses to type 2 thymus-independent antigens, were normal (Fig. 4 E). Loss of either Bmf or Bim also caused an abnormal increase in the numbers of mature B cells in inguinal lymph nodes, as well as an increase in the numbers of T1 B cells and mature B cells in the peripheral blood (Table I). Interestingly, loss of Bim caused a more pronounced accumulation of B lymphoid cells in blood and spleen than Bmf deficiency but in inguinal lymph nodes the numbers of B cells were higher in *bmf*$^{-/-}$ mice than in *bim*$^{-/-}$ mice (Table I).

These results indicate that Bmf-deficient B cell progenitors and/or mature B cells may have a survival advantage leading to their accumulation, B cell hyperplasia, and possibly also B cell neoplasia in older mice. To examine this hypothesis, we followed cohorts of WT and Bmf-deficient animals and assessed their B cell compartments at 12 mo of age. Consistent with our observations in young animals, spleens from Bmf-deficient animals were significantly increased when compared with spleens from age-matched WT or Puma-deficient animals (Table S1, available at http://www.jem.org/cgi/content/full/jem.20071658/DC1). The lymphadenopathy in *bmf*$^{-/-}$ mice, however, did not progress to B cell neoplasia, at least during our observation period of up to 18 mo (unpublished data).

To investigate possible consequences of the B cell excess observed in Bmf-deficient mice, we measured serum Ig levels in 8–10-wk-old mice and in animals challenged with antigen. Total serum Ig levels were significantly ($P < 0.0123$) elevated in *bmf*$^{-/-}$ mice, but this difference was no longer evident in aged (1-yr-old) animals (Fig. 5). Thus, Bmf deficiency may enhance development and/or survival of plasma cells at a young age, and this is consistent with the mildly elevated numbers of B220$^+$CD138$^+$ plasma cells found in spleens of young *bmf*$^{-/-}$ mice (Fig. 4 E). To test whether *bmf*$^{-/-}$ mice are able to mount normal immune responses, we challenged WT and Bmf-deficient mice with T cell–dependent

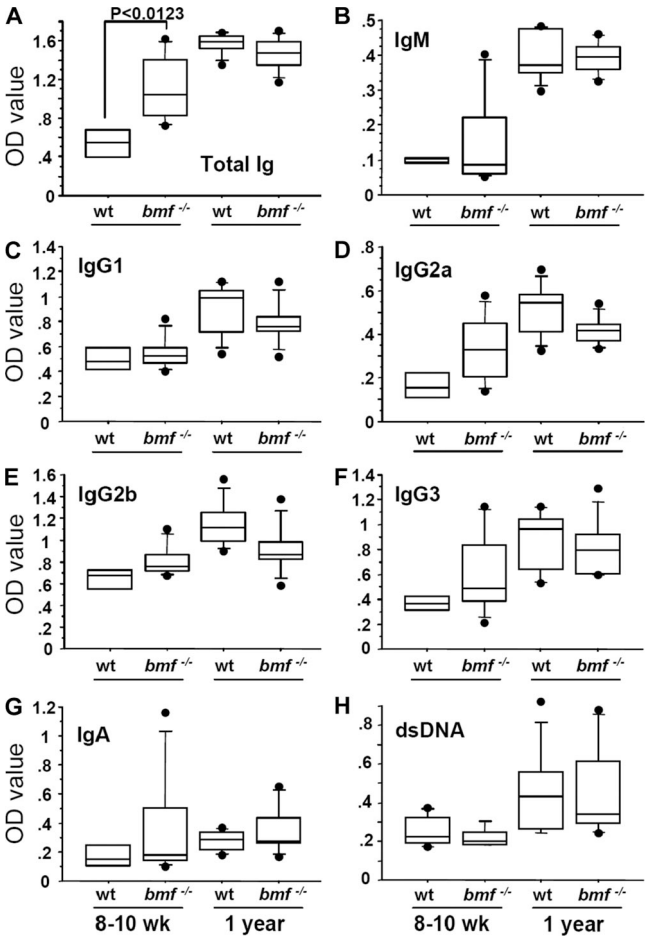

Figure 5. Mild hypergammaglobulinemia in untreated Bmf-deficient mice. Ig-titers in the sera from 8–12 wk or 12-mo-old WT and *bmf*$^{-/-}$ mice were quantified by ELISA. Dilutions were predetermined to produce absorbance readings in the linear range. Total Ig 1:80.000 (A), IgM 1:40.000 (B), IgG1 1:40.000 (C), IgG2a 1:4000 (D), IgG2b 1:80.000 (E), IgG3 1:40.000 (F), and IgA 1:40.000 (G). Box plots represent values from $n = 4$ WT and 8 *bmf*$^{-/-}$ mice (8–10 wk), and 8 WT and 8 *bmf*$^{-/-}$ aged mice. Significant differences were only observed in the total Ig levels between young WT and Bmf-deficient mice using Student's *t* test ($P < 0.0123$). (H) Autoantibodies to dsDNA were quantified in the sera from 8–12-wk- or 12-mo-old mice by ELISA using ds calf thymus DNA for coating (serum dilution 1:100). Box plots represent values from $n = 6$ WT and 6 *bmf*$^{-/-}$ mice (8–10 wk) and 5 WT and 8 *bmf*$^{-/-}$ aged mice.

(NP-OVA) (Fig. S2 A, available at http://www.jem.org/cgi/content/full/jem.20071658/DC1) and T cell–independent (TNP-Ficoll) antigens (Fig. S2 B). Quantification of antigen-specific Ig production did not reveal significant differences compared with WT mice, although IgG2a levels appeared to be slightly elevated in sera from Bmf-deficient mice (Fig. 2 D). To address the question whether loss of Bmf, similar to loss of Bim (16), facilitates the survival of autoreactive B cells, we also monitored animals for the presence of dsDNA-specific autoantibodies in sera from *bmf*$^{-/-}$ mice. Loss of Bmf did not trigger an accumulation of anti-dsDNA autoantibodies beyond the levels observed in age-matched WT mice (Fig. 5 H).

Bmf is a critical regulator of apoptosis in pre–B cells

The B cell hyperplasia observed in Bmf-deficient mice may be caused by defects in apoptosis at early or late stages of B cell development. To investigate this possibility, we analyzed cell death responses of purified B cells from *bmf*$^{-/-}$ and, for comparison, *puma*$^{-/-}$ animals. Immature bone marrow–derived pre–B cells and splenic B cells were isolated by cell sorting, placed in culture, and exposed to a broad range of apoptotic stimuli, including cytokine withdrawal, treatment with the glucocorticoid dexamethasone, the broad-spectrum kinase inhibitor staurosporin, the DNA-damaging drug VP16, the glycosylation inhibitor and ER stressor tunicamycin, and the HDAC inhibitors Trichostatin A, CBHA, or SAHA, as well as B cell receptor (BCR) ligation with cross-linking anti-IgM antibodies. Cell viability was monitored over time by AnnexinV-FITC/PI staining and flow cytometric analysis. Pre-B cells lacking Bmf were normally sensitive to spontaneous death in culture (Fig. 6 A), as well as death induced by VP16 (Fig. 6 C) but highly refractory to dexamethasone (Fig. 6 B), or HDAC-inhibition by SAHA (Fig. 6 D). B cells lacking Bmf, isolated from spleens by negative FACS-sorting (i.e., staining and depletion of T cells myeloid cells and erythroid cells) were as sensitive as WT cells to apoptosis induced by cytokine deprivation (Fig. S1 C), dexamethasone (Fig. S1 D), VP16 (Fig. S1 E), staurosporin, and tunicamycin (not depicted). Only SAHA-induced cell death showed delayed kinetics (Fig. S1 F). BCR ligation–induced apoptosis appeared somewhat delayed in the absence of Bmf, but this difference was not statistically significant (Fig. S1 F).

To test whether the reduced sensitivity to GC treatment in vitro may be of relevance in vivo, WT and Bmf-deficient mice were injected with graded doses of dexamethasone. Consistent with our in vitro observations, absence of Bmf provided pre–B cells with partial resistance to the effects of systemic GC injection (Fig. 6, E and F). Collectively, these results indicate that Bmf is critical for stress-induced apoptosis of pre–B cells, but appears to play only a modest or redundant role for stress-induced killing of mature B cells.

Assessment of viability of bone marrow–derived pre–B cells or mature splenic B cells straight after organ harvest revealed slightly higher percentages of viable (Annexin V-FITC/PI-negative) pre–B cells (mean viability WT 78.8 ± 5.6% vs. *bmf*$^{-/-}$ 89.1 ± 1.5%; $n = 4$) as well as mature IgM$^+$ B cells (mean viability WT 75.2 ± 3.4% vs. *bmf*$^{-/-}$ 82.8 ± 2.0%; $n = 4$) in the absence of Bmf. Interestingly, we observed that the percentage of BrdU$^+$ cycling pro–/pre–B cells was lower in the bone marrow of *bmf*$^{-/-}$ mice (10.42 ± 2.42%) when compared with the relevant WT (16.35 ± 0.64%) control mice ($n = 4$; $P = 0.008$). However, in vitro proliferative responses of isolated pre–B cells stimulated with SCF and IL-7 or mature splenic B cells stimulated by anti-CD40 antibodies, BCR-ligation, LPS, or CpG were normal in the absence of Bmf (Fig. S6 and not depicted).

Collectively, these data indicate that loss of Bmf confers a survival advantage to B lineage cells in vivo and that the

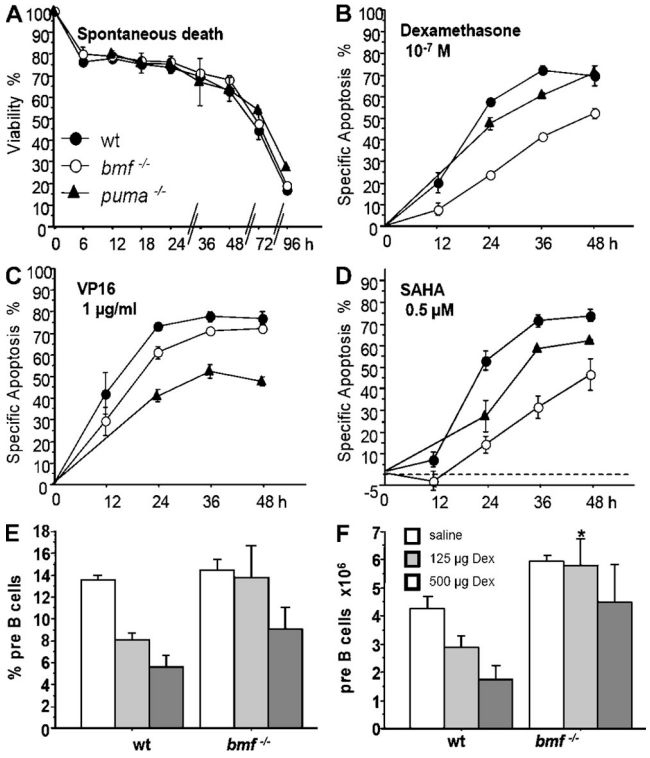

Figure 6. Impaired cell death responses in *bmf*$^{-/-}$ pre–B cells. FACS-sorted pre–B cells (B220$^+$sIgM$^-$CD43$^-$) from mice of the indicated genotypes were put in culture without further treatment (A; spontaneous death) or exposed to dexamethasone (B), the DNA-damaging drug VP16 (C), or the HDAC-inhibitor SAHA (D). Cell death was monitored, and the extent of apoptosis induced specifically by different stimuli was calculated as indicated in Fig. 3. Means ± the SEM from four independent experiments and $n = 5$ animals per genotype are shown. Significant differences in cell death induction were observed between WT and Bmf-deficient cells treated with dexamethasone ($P = 0.0001$) or SAHA ($P = 0.004$) using ANOVA analysis. Mice of the indicated genotypes were injected with graded doses of dexamethasone and the percentage (E) and total number (F) of surviving pre–B cells was assessed 20 h later by cell counting of bone marrow single-cell suspensions and flow cytometric analysis of pre–B cell surface marker expression (B220$^+$sIgM$^-$CD43$^-$). Bars represent the means ± the SEM of ≥3 animals per genotype/dose (three independent experiments). Significant differences in vivo were observed between the number of surviving WT and Bmf-deficient pre B-cells in mice treated with 125 µg dexamethasone ($P = 0.01$).

accumulation of mature B cells in peripheral organs, caused by loss of Bmf, may cause a reduction in the proliferation of B cell precursors in the bone marrow as a negative feedback.

Bmf regulates B cell homeostasis in vivo

The observation that spontaneous death of immature and mature B cells in culture was not significantly different between WT and Bmf-deficient cells, whereas the percentage of viable cells appeared higher in *bmf*$^{-/-}$ mice in vivo, made us wonder whether the observed B cell accumulation was caused by a cell-intrinsic apoptosis defect caused by loss of Bmf, or whether Bmf deficiency–induced changes in the microenvironment may be responsible for this phenomenon. Therefore, we set up competitive reconstitution experiments in which lethally irradiated congenic Ly5.1 recipient mice were reconstituted with a 50:50 mix of either WT Ly5.1 and Ly5.2 bone marrow cells or a 50:50 mix of WT Ly5.1 and *bmf*$^{-/-}$Ly5.2 bone marrow cells. Immunofluorescent staining and FACS analysis showed that WT and *bmf*$^{-/-}$ mice had similar numbers of Lin^{-}Sca-1^{+}c-kit^{+} cells in their bone marrow (mean WT 3.5 vs. 3.7%; $n = 3$). Hemopoietic reconstitution was followed over time by assessing the percentages of Ly5.2^{+} cells in the peripheral blood (Fig. 7, A–D), and in thymus and spleen, reconstitution was assessed at a single time point, which was after 21 wk (Fig. 7, E and F). In the irradiated hosts, some of the leukocyte subsets contained significantly more cells that were derived from *bmf*$^{-/-}$ stem cells than from WT stem cells. Among the CD4^{+} T lymphocytes and CD19^{+} B lymphocytes in reconstituted hosts there was a clear predominance of cells of *bmf*$^{-/-}$ origin (Fig. 7, B and D). Numbers of Bmf-deficient CD8^{+} T cells were, if anything, only slightly increased compared with CD8^{+} cells of WT origin (Fig. 7 C). Interestingly, a percentage significantly greater than the expected 50% of immature CD4^{+}8^{+} cells, as well as CD4^{+}8^{-} and CD4^{-}8^{+} T cells in thymi of reconstituted animals, were of *bmf*$^{-/-}$ origin (Fig. 7 E). Moreover, consistent with our findings in peripheral blood, the percentages of mature CD4^{+} T cells and CD19^{+} B cells lacking Bmf was significantly increased above the expected 50% in the spleen and lymph nodes (Fig. 7 F and not depicted). Collectively, these data demonstrate that absence of Bmf provides a significant cell autonomous survival advantage to the B linage cells and, to a lesser extent, to developing and mature T lymphocytes.

Bmf is not required for apoptosis induced by UV irradiation or cell detachment

As shown in Fig. 1 C, *bmf* mRNA was detected in MEFs, and Bmf and Bim proteins were previously shown to be released from cytoskeletal sequestration in response to UV-irradiation or loss of integrin signaling during anoikis (22, 23). To investigate

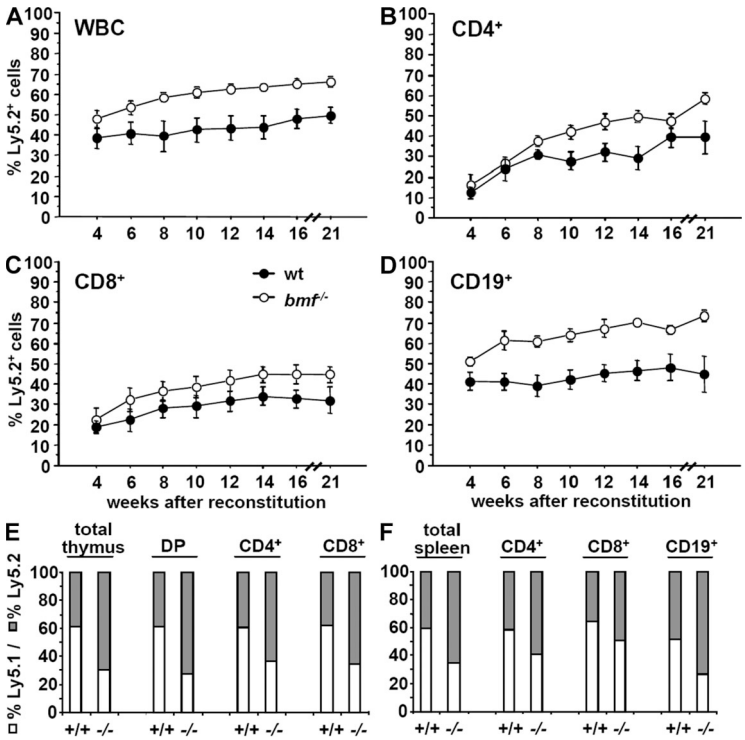

Figure 7. Bmf-deficiency promotes abnormally enhanced lymphocyte accumulation through a cell autonomous mechanism. Ly5.1 congenic mice were reconstituted 6 h after lethal irradiation (10 Gy) using a 50:50 mixture of WT Ly5.1 + WT Ly5.2 or WT Ly5.1 + *bmf*$^{-/-}$Ly5.2 bone marrow cells (total 4 × 10^{6} cells/mouse). Reconstitution was monitored over time by evaluating the percentage of donor cells in peripheral blood by FACS analysis using a Ly5.2-specific antibody, either alone (A) or in combination with the T cell markers CD4 (B), CD8 (C), or the B cell marker specific antibody CD19 (D). 21 wk after reconstitution, animals were killed and the percentage of donor-derived lymphocytes was assessed in thymus (E) and spleen (F) using the cell surface marker–specific antibodies indicated.

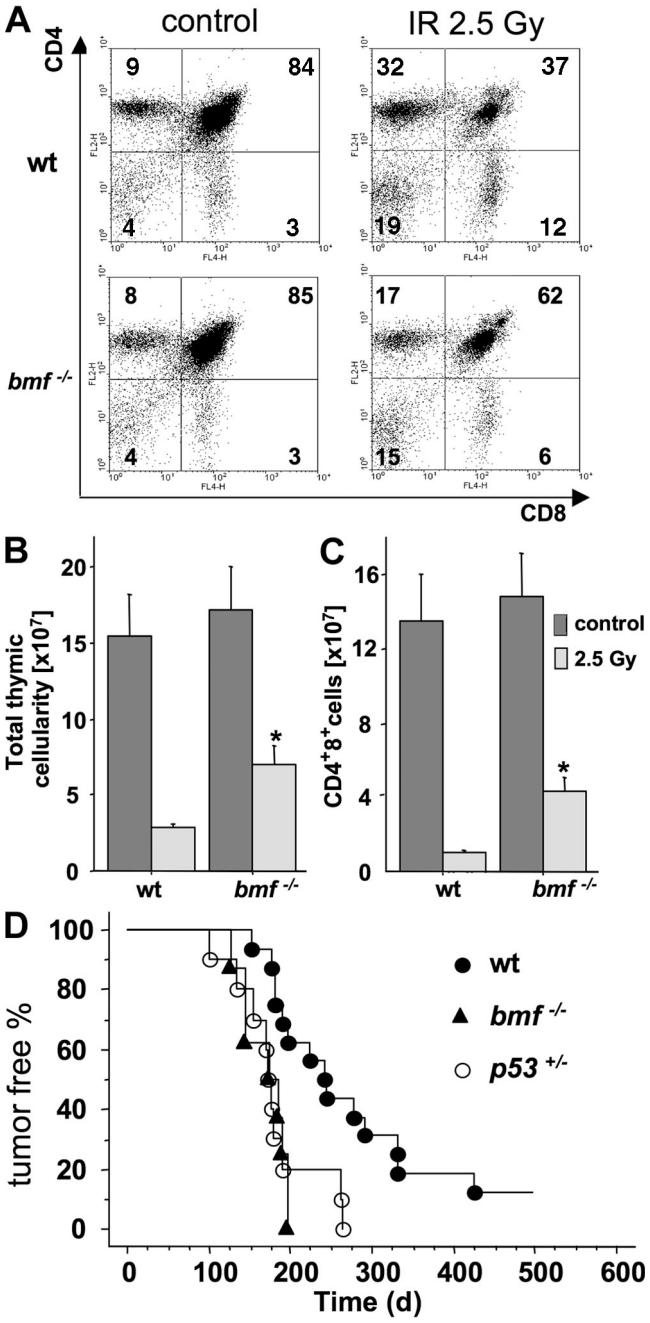

Figure 8. Loss of Bmf enhances γ irradiation induced thymic lymphoma development. Mice of the indicated genotypes (7–8 wk of age) were exposed to whole body irradiation using 2.5 Gy. Animals were killed 20 h later, and thymocyte numbers were evaluated by FACS analysis of cell surface marker expression (A) and cell counting to calculate the total number of thymocytes (B) and $CD4^+8^+$ immature thymocytes (C). Bars represent means ± the SEM of 3 WT and 5 Bmf-deficient animals and two independent experiments. Significant differences in depletion of total thymocytes (P = 0.0044) and $CD4^+8^+$ thymocytes (P = 0.003) were confirmed using ANOVA analysis. Cohorts of WT (n = 16), $bmf^{-/-}$ (n = 8), and $p53^{+/-}$ (n = 9) mice were exposed to a fractionated γ irradiation protocol (4 × 1.75 Gy in weekly intervals, starting at 4 wk of age) and monitored for the development of thymic lymphomas over time. (B) Kaplan-Meier analysis of tumor-free survival of mice of the indicated genotypes. Log rank (Mantle-Cox) analysis was used to calculate differences between WT and $p53^{+/-}$ (P = 0.027) and WT and $bmf^{-/-}$ mice (P = 0.009).

the requirement of Bmf for pathways to apoptosis, we exposed low-passage primary MEFs from WT mice or mice lacking the BH3-only proteins Bmf or Bim to graded doses of UV irradiation and analyzed survival over time in culture (Fig. S3, A and B). Annexin V-FITC/PI staining and flow cytometric analysis of cells revealed that neither absence of Bmf nor Bim consistently prevented cell death in response to UV irradiation (Fig. S3, A and B).

Primary MEFs were subjected to anoikis by culturing them on poly-hema–coated plates, thereby preventing their attachment and simulating loss of contact to extracellular matrix, in the presence or absence of serum. Loss of Bmf did not delay cell death by anoikis, regardless of serum conditions (Fig. S2, C and D). To confirm this finding in a more physiologically relevant setting we used differentiated epithelial cells lining the gut lumen. Epithelial cells from the small and large intestine are expelled from the tip of villi at high frequency and are subsequently replaced by new differentiating cells derived from stem cells located at the basis of the crypts. Mature cells that are shed are thought to die by anoikis caused by lack of integrin signaling and/or loss of contact to the extracellular matrix (32). Because we detected *bmf* mRNA expression in the colon (23), we started to assess the role of Bmf in anoikis induction of gastrointestinal epithelial cells. Primary epithelial cells were isolated from the small intestine and/or colon of WT, $bmf^{-/-}$, or $bim^{-/-}$ animals. Purity of the isolated cell suspensions was verified by intracellular staining for the epithelial cell marker cytokeratin using a pan-cytokeratin–specific antibody and flow cytometric analysis (Fig. S4 A). Isolated cell suspensions derived from the small intestine routinely contained >80% epithelial cells, and those from the colon contained >90% epithelial cells (Fig. S4 A). Isolated epithelial cells were cultured in low attachment plates, and viability was monitored over time. Flow cytometric staining of DNA content (cells with a sub-G1 DNA content being considered apoptotic) and intracellular staining for active caspase-3 demonstrated that epithelial cells undergo rapid, caspase-dependent apoptosis in vitro. However, this cell death was not attenuated in the absence of Bmf or Bim (Fig. S4 B). Statistical analysis of combined experiments on colonic epithelial cells (Fig. S4 C) or cells from the small intestine (Fig. S4 D) failed to reveal significant differences between the genotypes, although cell death appeared somewhat delayed in colonic epithelial cells lacking Bim or Bmf. Collectively, our data show that Bmf and Bim are dispensable for anoikis of gastrointestinal epithelial cells.

Loss of Bmf enhances γ irradiation–induced thymic lymphoma development

The human *BMF* gene is encoded on chromosome 15q14, a region that harbors a potential tumor suppressor that is frequently lost during the late stages of lung and breast cancer (25).

To examine the tumor suppressor capacity of Bmf, we exposed a cohort of WT, *bmf*$^{-/-}$, and *p53*$^{+/-}$ animals to a fractionated γ irradiation protocol and monitored the development of thymic lymphomas over time. Interestingly, loss of Bmf delayed cell death of thymocytes in response to γ irradiation in vivo (Fig. 8, A and B) and markedly accelerated the onset of thymic lymphomas to an extent comparable to the effect caused by loss of one allele of *p53* (Fig. 8 C). The thymic lymphomas arising in *bmf*$^{-/-}$ mice displayed either an immature CD4^{+}8^{+} or CD8^{+} SP phenotype, with frequent infiltrations of tumor cells seen in the spleen (Fig. S5). Our findings are consistent with the notion that BH3-only proteins can act as tumor suppressors, and they document a so far unknown role for Bmf in DNA damage-induced apoptosis and suppression of thymic lymphoma development.

DISCUSSION

Studies on BH3-only protein knockout mice have started to unravel cell-type and death stimulus-specific functions in apoptosis signaling for most members of this family. Loss of individual BH3-only proteins, with the exception of Bim (9), is generally compatible with embryonic development suggesting redundancy among these proteins in developmental cell death. In the adult organism, however, cell type- as well as death stimulus–specific defects have been reported in some knockout mouse strains lacking individual BH3-only protein genes (1). Bid-deficient mice, for example, resist Fas-mediated hepatocyte destruction, supporting its role as a link to and amplifier of the death receptor-signaling pathway (11, 12). In contrast, lymphocytes and other cell types from mice lacking *puma* show a profound defect in p53-induced apoptosis in response to DNA damage. Loss of Bim renders leukocytes refractory to the effects of cytokine deprivation, deregulated Ca^{2+}-flux and glucocorticoids and strongly interferes with the deletion of autoreactive T and B cells (17–19), as well as the proper termination of immune responses (20, 21). Interestingly, Bim and Puma synergize in the mediation of many forms of cell death because lymphocytes from *bim*$^{-/-}$*puma*$^{-/-}$ mice resist p53-dependent and -independent forms of apoptosis more potently than cells from single knockout mice (16). Moreover, although loss of *Blk* on its own does not cause any overt abnormalities, the combined loss of Blk and Bim leads to male infertility caused by defects in spermatogenesis (10, 33).

Our analysis of Bmf-deficient animals revealed several novel and unexpected findings. We found that Bmf is dispensable for embryogenesis and organogenesis, which is consistent with the observation in all other BH3-only knockout mouse models investigated thus far, with the exception of the partial embryonic lethality caused by loss of Bim. Surprisingly, we noted that loss of Bmf specifically causes a defect in B cell homeostasis, whereas T cell and myeloid cell development and homeostasis were not affected (Table I). The numbers of bone marrow pre–B cells and transitional B cells were both found to be abnormally elevated in Bmf-deficient animals (Table I). So far, the death of B cell progenitors in the bone marrow caused by loss of cytokine support has been considered to depend mostly on Bim because loss of Bim can partially rescue the B cell lymphopenia caused by IL-7 or -7R deficiency (34, 35). Interestingly, only the number of naive and recirculating mature B cells was significantly elevated in *bim*$^{-/-}$ mice (9, 36). However, the numbers of these B cell populations were reported to be even higher in *vav-bcl-2 tg* mice (16), suggesting that other BH3-only proteins besides Bim can also regulate the developmentally programmed death of these cells. It is interesting to note that B cell numbers in the bone marrow of *bim*$^{-/-}$*puma*$^{-/-}$ (16), *bim*$^{-/-}$*blk*$^{-/-}$ (10), or *bim*$^{-/-}$*bad*$^{-/-}$ (unpublished data) double-deficient mice do not exceed that observed in *bim*$^{-/-}$ mice. This excludes overlapping functions for Bim with Puma, Blk, or Bad in the regulation of B cell apoptosis in the bone marrow, and indicates that Bmf is a likely candidate that may have overlapping functions with Bim in this process. Interestingly, pro–B cell numbers were the only B cell subset not affected by the absence of Bmf, which is consistent with the lack of its expression in theses cells (Fig. 2). Bmf was found to be expressed at high levels in all other B cell subsets investigated, but comparatively lower levels were found in mature splenic T cells (Fig. 2 A), which is consistent with the finding that the number of T cells was normal in the absence of Bmf (Table I).

The splenomegaly observed in *bmf*$^{-/-}$ mice was clearly less pronounced than that observed in *bim*$^{-/-}$ animals because of the fact that loss of *bmf* caused only accumulation of B cells, but not T cells, whereas loss of Bim caused accumulation of both cell types (Table I). Consistent with our hypothesis that Bim and Bmf co-regulate developmental death of B cells, the numbers of splenic B cells in *vav-bcl-2 tg* mice also clearly exceed those observed in Bim-deficient mice (16). It will therefore be interesting to see whether compound mutants that lack both Bim and Bmf show a synergistic increase in B cell numbers or other leukocyte subsets.

Loss of Bmf interfered most potently with apoptosis in thymocytes and pre–B cells induced by glucocorticoids or inhibitors of histone-deacetylases. The finding that *bmf*$^{-/-}$ lymphoid cells are abnormally resistant to glucocorticoid-induced apoptosis is consistent with the observation that *bmf* expression is induced by systemic application of dexamethasone in children suffering from acute lymphatic leukemia and in corresponding model cell lines in vitro (28). The involvement of Bmf in HDAC inhibitor–induced cell killing confirms previously published data gathered in oral and esophageal squamous carcinoma cells, which suggested that Bmf may be rate limiting for the antineoplastic effects of these drugs (24). Surprisingly, cell death triggered by CBHA was only mildly delayed in *bmf*$^{-/-}$ thymocytes and Trichostatin A induced cell death as potently as in WT cells (Fig. S1, A and B), arguing against a unifying cell death mechanism triggered by HDAC inhibitors, as suggested by others (37). In contrast to published data, we were unable to observe a significant increase in Bmf protein expression after exposure to SAHA (Fig. 3 F and not depicted), demonstrating that increased Bmf expression is not a prerequisite to kill primary lymphocytes by this HDAC inhibitor. The differences observed may be caused by changes

in *bmf*-gene accessibility in primary versus transformed cells. In malignant cells, *bmf* may be silenced epigenetically, a possibility that may be relevant here because the *bmf* gene contains a well-defined CpG island in its promoter region (24).

The basis for the abnormal accumulation of pre–B cells and mature B cells in the absence of Bmf is unclear at present. Bmf as a target for BCR or cytokine receptor signaling does not appear to be a likely explanation because application of IL-7 or BAFF potently extended the survival of pre–B and mature B cells, respectively (not depicted). Moreover, BCR ligation-induced apoptosis was normal in the absence of Bmf (Fig. S1 F). On the other hand, the apoptosis defect of lymphocytes appears to be cell intrinsic, as documented in our reconstitution experiments (Fig. 6). We also excluded enhanced proliferation potential of Bmf-deficient B cells in response to mitogens as a possible explanation for the observed B cell hyperplasia (Fig. S6 and not depicted). The observed resistance to experimentally applied glucocorticoids (in vitro and in vivo) may indicate that B cell accumulation is a consequence of the abnormal resistance of $bmf^{-/-}$ B cells to endogenous glucocorticoids or related hormones. It is theoretically possible that Bmf loss renders B cells resistant to death stimuli that operate at developmental checkpoints, such as apoptosis caused by lack of pre–BCR or BCR expression. This hypothesis can best be analyzed by generating mice with defects in BCR gene rearrangement (e.g., $rag\text{-}1^{-/-}$ or *scid* mice) that also lack Bmf.

We have previously shown that Bmf changes its subcellular location after UV irradiation in MCF-7 cells, and therefore anticipated that it may play a role in the cellular response to UV-induced DNA damage (23). However, using primary MEFs, we observed that loss of *bmf* did not interfere with cell death induced by UV irradiation. We, and others, have previously demonstrated that the p53-regulated BH3-only protein Noxa is the major rate-limiting factor in UV irradiation–induced apoptosis of primary and *E1A/ras*-transformed MEFs (38, 39). In contrast, cells lacking Bim, Puma, or Bad were all normally sensitive to UV irradiation and, remarkably, combined loss of Noxa and Puma did not afford better protection than loss of Noxa alone. Interestingly, these studies also revealed that overexpression of Bcl-2 provided greater protection against UV than loss of Noxa, indicating that additional BH3-only proteins may become activated in this process (39). Although loss of Bmf alone has no effect on UV irradiation–induced apoptosis (Fig. S2, A and B), it may still collaborate with Noxa in this cell death pathway, and in this regard it may be interesting to note that Bmf and Noxa have complimentary specificities of binding to prosurvival Bcl-2 family members (7, 8).

Anoikis induction prevents epithelial cells from colonizing ectopic sites, and resistance to anoikis is thought to be a prerequisite for tumor cells to metastasize (32). Expression of mutated Ras^{V12} can prevent anoikis induction in a series of breast cancer cell lines and primary mammary epithelial cells. The molecular basis for this phenomenon appears to be the maintenance of Bcl-x_L expression levels with concomitant suppression of the proapoptotic activity of Bak (40, 41), plus inhibition of Bim through MAPK-mediated proteasomal degradation (42, 43). It has, however, been argued that Bim primarily senses the loss or lack of EGF-R–mediated ERK activation and that loss of integrin signaling may activate other proapoptotic molecules besides Bim (44, 45). Bmf was a good candidate for such a molecule because it changes its subcellular localization in MCF-7 cells that were forced to undergo anoikis (23). However, our analysis of primary MEFs and gastrointestinal epithelial cells derived from the small intestine or colon did not support a rate-limiting role for Bmf or Bim in this process. This does not exclude a role for either protein in anoikis of primary mammary epithelial cells, as previously suggested (46), or in transformed cell lines (23).

The fact that loss of Bmf accelerated thymic lymphomagenesis triggered by repeated γ irradiation is consistent with its proposed role as tumor suppressor (23). The fact that Bmf deficiency can also delay γ irradiation–induced apoptosis in thymocytes is surprising because we did not find evidence that *bmf* is induced in response to DNA damage (unpublished data). However, similar observations have been made in Bim-deficient mice (30). Our findings suggest that Bmf may act in a parallel p53-independent pathway to apoptosis that is activated by DNA damage, or that it may be activated by latent oncogenic stress subsequent to the pathological response to DNA damage.

Collectively, our investigations have revealed a prominent role for Bmf in lymphocyte apoptosis induced by glucocorticoids and HDAC inhibitors, as well as a role as tumor suppressor. In addition, our data indicate that Bmf acts in concert with Bim to regulate B cell homeostasis and lymphocyte apoptosis, and investigations on animals lacking Bim and Bmf are underway to examine this.

MATERIALS AND METHODS

Generation of Bmf-deficient mice and other mouse strains used. All animal experiments were performed in accordance with the Austrian "Tierversuchsgesetz" (BGBl. Nr. 501/1988 i.d.g.F) and have been granted by the Bundesministerium für Bildung, Wissenschaft und Kultur (bm:bwk) or were performed according to the guidelines of the Melbourne Directorate Animal Ethics Committee. The generation and genotyping of the Puma- and Bim-deficient mice has been previously described (9, 13). The $puma^{-/-}$ mice were generated on an inbred C57BL/6 genetic background using C57BL/6-derived ES cells. The $bim^{-/-}$ mice were originally generated on a mixed C57BL/6 × 129SV genetic background, using 129SV-derived ES cells, and they were subsequently backcrossed onto the C57BL/6 background for at least 12 generations.

To generate a *bmf*-targeting construct, C57BL/6 genomic DNA was isolated and subcloned from the RPCI-23 BAC clone # 266K3 (Roswell Park Cancer Institutes, Roswell Park, NY), harboring the entire *bmf* locus (Fig. 1). After electroporation and selection of C57BL/6-derived Bruce4 ES cells, two out of three homologous recombined clones were injected into BALB/c blastocysts and delivered by CD1 surrogate mothers to generate chimeric mice. Heterozygous offspring of subsequent mating of chimeric males, which were derived from two independent ES cell clones, with C57BL/6 females were used to establish the $bmf^{f/+}$ mouse lines, designated 372 and 376, containing a floxed *bmf*-allele. The neomycin resistance cassette and exons 3 and 4 of the *bmf* gene (Fig. 1 A) were subsequently deleted by crossing to female C57BL/6 *ubi-cre* deleter mice to establish the substrains 372del and 376del. These animals were further backcrossed with C57BL/6

mice to breed out the *cre* transgene. All analyses reported were performed using 376del mice and, where possible, all findings were also confirmed using 372del mice.

Cell culture and reagents. Primary hemopoietic cells were cultured in RPMI 1640 medium (PAA), 250 μM L-glutamine (Invitrogen), 50 μM 2-mercaptoethanol, nonessential amino acids (Invitrogen), penicillin/streptomycin (Sigma-Aldrich) and 10% FCS (PAA). For the induction of cell death, the following reagents were used: FLAG epitope-tagged FasL (Alexis) at 100 ng/ml, together with cross-linking M2 anti-FLAG antibody (Sigma-Aldrich) at 1 μg/ml, staurosporine (Sigma-Aldrich) at 100 nM, ionomycin (Sigma-Aldrich) at 1 μg/ml, PMA at 10 ng/ml (Sigma-Aldrich), VP16 (Sigma-Aldrich) at 1 or 10 μg/ml, the ER stressor tunicamycin (Sigma-Aldrich) at 10 μg/ml, and the glucocorticoid dexamethasone at 10^{-6} or 10^{-7} M (Sigma-Aldrich). Trichostatin A (Sigma-Aldrich), CBHA (Calbiochem), or SAHA (a gift from R. Johnstone, Peter MacCallum Cancer Center, Melbourne, Australia). Injections of saline, 125 μg dexamethasone, or 500 μg dexamethasone (Dexabene; ratiopharm) were performed i.p. in a final volume of 200 μl.

MEFs were derived from embryonic day 14.5 embryos and isolated after removal of internal organs, brain, and fetal liver by trypsin digestion of the remaining tissue. All experiments were performed using early passage (<5) MEFs. MEFs were cultured in the high-glucose version of Dulbecco's modified Eagle's (DME) medium supplemented with L-glutamine, 10% FCS, and antibiotics.

Isolation of primary small intestinal and colonic epithelial cells. Complete small intestine and colon were dissected from mice, freed from residual feces and mucus after longitudinal section, and transferred into ice-cold HBSS without Ca^{2+} and Mg^{2+}. After rinsing several times in HBSS (Invitrogen) at room temperature, residues were shaken gently in 15 ml of HBSS containing 2 mM EDTA, pH 8.0, for 30 min at 37°C. The solid material was transferred to a new 50-ml tube, and the supernatant was discarded. The remaining mucosa was vortexed in 10 ml PBS, and the supernatant containing complete crypts and some single cells was collected into a fresh 15-ml tube containing PBS. Vortexing was repeated until the supernatant was almost clear. To separate remaining crypts from single cells, crypts were allowed to settle down for up to 5 min at room temperature, and single cells were transferred by carefully pipetting the supernatant into a new 15-ml tube and collected by centrifugation at 1,500 rpm for 5 min at room temperature. After washing with PBS, the cells were resuspended in keratinocyte serum–free medium (KFS) supplemented with EGF and BPE (Invitrogen). To induce anoikis, cells were transferred to a low adherence 6-well plate and incubated at 37°C for the indicated time. Cell viability was assessed by intracellular DNA content analysis in a FACScan (BD Biosciences), as described in Cell death assays.

Immunoblotting. Western blotting was performed as previously described (47). Membranes were probed with rabbit anti-Puma antiserum (Cell Signaling Technology), monoclonal antibodies to Bad (Cell Signaling Technology), active caspase-3 (Cell Signaling Technology), rat anti–mouse Bmf mAb (17A9) or rat anti–mouse, rat, human, monkey, dog Bim (3C5), generated at the WEHI and now commercially available from Alexis. Equal loading of proteins was confirmed by probing filters with antibodies specific for β-actin (Sigma-Aldrich) or ERK1/2 (Cell Signaling Technology). Horseradish peroxidase–conjugated sheep anti–rat Ig antibodies (Jackson ImmunoResearch Laboratories) or goat anti–rabbit antibodies (DAKO) served as secondary reagents, and the enhanced chemiluminescence (GE Healthcare) system was used for detection.

BrdU staining. BrdU (Roche) was injected i.p. (1 mg/mouse in 200 μl saline) 4 h before sacrifice of the animals. BrdU incorporation was quantified according to the recommendations of the BrdU Flow kit staining protocol (Becton Dickinson) using a FITC-labeled anti-BrdU mAb (Roche) in combination with fluorochrome-conjugated antibodies against CD4, CD8, Thy1, CD19, IgM, and CD43. Thymocytes from untreated mice were routinely included in the analysis and served as a negative control.

Cell death assays. The percentage of viable cells in culture was determined by staining with 2 μg/ml PI plus FITC-coupled Annexin V (Becton Dickinson) and analyzing the samples in a FACScan (Becton Dickinson). Gastrointestinal epithelial cells were fixed overnight at 4°C in 70% ethanol and stained for 20 min at 37°C with 69 μM PI in 38 mM sodium citrate, pH 7.4, containing 5 μg/ml RNase A. Between 5,000 and 10,000 cells were analyzed in a FACScan. Apoptotic cells were identified within the PI-stained population by virtue of exhibiting an apparent subdiploid DNA content.

Northern blotting, Southern blotting, and PCR analysis. PolyA$^+$ mRNA was isolated from embryonic day 14.5-derived MEFs and NIH-3T3 cells using Trizol reagent (Invitrogen) and subsequent enrichment using an mRNA isolation kit (QIAGEN). 3–4 μg of polyA$^+$ mRNA were size fractioned by electrophoresis on a denaturing 1% agarose-formaldehyde gel, transferred overnight in 10× SSC onto Hybond N nylon membranes (GE Healthcare), UV cross-linked, baked at 80°C for 2 h, and probed with a ^{32}P-labeled mouse *bmf* cDNA probe (bp 1–558 of *bmf*) in CHURCH buffer over night at 65°C. Membranes were washed in 40 mM Na-phosphate buffer containing 1% SDS at room temperature and exposed in a phosphorimager for 4 d.

To confirm correct targeting of ES cells and deletion of the *bmf* gene in tissues, 20 μg of total genomic DNA was digested with the appropriate restriction enzymes over night. Samples of DNA were size fractioned in 0.8% agarose gels in TAE buffer, depurinated in 0.25 M HCl, denatured in 0.4 M NaOH, and transferred in the same buffer onto Hybond N$^+$ nylon membranes. Filters were probed with 5′ and 3′ external probes or a neomycin cassette-specific probe in CHURCH buffer at 65°C overnight. Membranes were washed in 40 mM Na-phosphate buffer containing 1% SDS at 65°C and exposed in a phosphorimager for up to 2 d.

Littermates from heterozygous (*bmf*$^{+/-}$) intercrosses were genotyped by PCR using primer pairs specific for the WT or the targeted *bmf* allele and the following cycle conditions: 4 min at 94°C; 40 s at 94°C, 30 s at 55°C, and 60 s at 72°C (30 cycles); and 5 min at 72°C. WT allele primers: forward, 5′-GGAGTTCAGACTTCGCCGAGAG-3′, and reverse 5′-GGCTGGTCACAAAGTTTGACACTG-3′ (220 bp product); primers for the targeted allele: forward 5′-GGAGTTCAGACTTCGCCGAGAG-3′ and reverse 5′-GCAAGAGGCAAGCCCTTCACTTGG-3′. The WT and targeted *bmf* alleles were amplified in separate reactions, yielding PCR products of 220 and 600 bp size, respectively.

Immunofluorescence staining, flow cytometric analysis, and cell sorting. Single-cell suspensions from peripheral blood, bone marrow, lymph nodes, spleen, and thymus were surface stained with monoclonal antibodies conjugated with FITC, R-PE, allophycocyanin, or biotin (Invitrogen). The monoclonal antibodies used, and their specificities, are as follows: RA3-6B2, anti-B220; GK1.5, anti-CD4; YTS169, anti-CD8; RB6-8C5, anti-Gr-1; R2/60, anti-CD43; 5.1, anti-IgM; 11/26C, anti-IgD; MI/70, anti-Mac-1; Ter119, anti-erythroid cell surface marker; T24.31.2, anti-Thy-1; IM7, anti-CD44; H57-59, anti-TCRβ; anti-CD19, MB19-1 (all eBioscience); 7G6, anti-CD21; B3B4, anti-CD23; 281–2, anti-CD138 (all Becton Dickinson). Biotinylated antibodies were detected using streptavidin-RPE (DAKO) or streptavidin-vPE-Cy7 (Becton Dickinson). Flow cytometric analysis was performed using a FACSCalibur cell analyzer (BD Biosciences). Sorting of cells was performed using a FACSVantage cell sorter (Becton Dickinson).

Quantification of total immunoglobulin and autoantibody levels. Ig-titers in the serum from 8–12-wk-old mice were quantified using an Ig clonotyping system, according to the manufacturer's instructions (Southern-Biotech). Serum samples were used in a dilution range from 1:4,000 to 1:160,000, depending on the isotype to secure absorbance readings in a linear range. 6–8-wk-old WT and *bmf*$^{-/-}$ mice were injected i.p. with NP-OVA (100 μg/mouse in CFA) to induce T cell–dependent humoral responses or were injected with 10 μg/mouse TNP-Ficoll in PBS (Biosearch Technologies) to induce TI-2 humoral responses. Blood was collected from the retro-orbital plexus either before immunization or at day 7, 14, and 21 after immunization using a heparinized capillary, collected in an Eppendorf tube,

and incubated for 2–3 h at 37°C. The samples were centrifuged, and serum was obtained and stored at −80°C. To determine antibody titers against 4-hydroxy-3-nitrophenylacetyl (NP) and 2,4,6-trinitrophenyl (TNP) the respective antigen conjugated to BSA (Biosearch Technologies) was coated on ELISA plates. ELISAs were performed as described (16). Serum samples were used in a dilution range from 1:800 to 1:1,600. To detect anti-ds DNA-specific antibodies, calf thymus DNA (Sigma-Aldrich) in distilled water. (12.5 μg/ml) was allowed to bind overnight to 96-well ELISA plates (Corning Costar) precoated for 1 h at 37°C with poly-L-lysine (0.1% in distilled water). For anti-dsDNA autoantibody detection, a horseradish peroxidase–labeled goat anti–mouse IgH + L-specific antibody and ABTS as a substrate were used (Souther Biotech). Mouse sera were diluted 1:100 in PBS/BSA1%. Serum derived from autoimmune prone NZW/NZW F1 mice was used as a positive control.

Cell proliferation assays. FACS-sorted splenic B cells (10^5/well) were cultured in the presence of saturating concentrations of IL-2, -4, and -5 (all from PeproTech) without further treatment or were stimulated with 2 μg/ml goat anti–mouse IgM $F(ab')_2$ fragments (Jackson ImmunoResearch Laboratories), 20 μg/ml LPS (Sigma-Aldrich), 2 μg/ml hamster anti–mouse CD40 mAb (HM40-3; BD), or 100 nM of ODN74, a CpG motif containing oligodeoxynucleotide (5′-AAAAAAAAAAAAAACGTTAAAAAAAAAAA-3′). Cells were pulsed for 18 h with 1 μCi/well [^{3}H]thymidine (GE Healthcare) at day 2 and 4, respectively. Alternatively, cells were labeled with CFSE (Invitrogen) at day 0, and loss of fluorescence intensity was assessed by flow cytometry after 48 or 72 h in culture in the absence or presence of mitogens. In brief, total splenic B cells, isolated by negative FACS sorting, were washed twice in PBS and incubated in 5 μM CFSE/PBS solution for 10 min at 37°C. Cells were washed immediately three times in excess PBS and put in culture. FACS-sorted pre–B cells derived from bone marrow (10^5/well) were cultured in the absence or presence of graded doses of IL-7 (PeproTech), and proliferation was monitored by FACS analysis quantifying changes in cell size in the FSC profile over time.

Competitive hemopoietic reconstitution assays. C57BL/6 Ly5.1 coisogenic animals were purchased from Charles River Laboratories and exposed to a single dose of γ irradiation (10Gy). Mice were reconstituted i.v. 6 h later using a 50:50 mixture of WT Ly5.1 + WT Ly5.2 or WT Ly5.1 + *bmf*$^{-/-}$ Ly5.2 bone marrow cells (total 4×10^6 cells/mouse). Treated mice received 2 mg/ml neomycine in the drinking water for 4 wk after reconstitution to minimize the risk of infection. Reconstitution was monitored in peripheral blood samples over time by FACS analysis using a Ly5.2-specific antibody either alone or in combination with antibodies to CD4, CD8, or CD19.

Preparation of histological sections. Organs were fixed in 4% paraformaldehyde in PBS, processed according to standard procedures, and stained in hematoxylin and eosin.

Statistical analysis. Statistical analysis was performed using the unpaired Student's *t* test or analysis of variance analysis, where indicated, and applying the Stat-view 4.1 software program. P values of <0.05 were considered to indicate statistically significant differences.

Online supplemental material. Fig. S1 shows that loss of Bmf does not generally impair apoptosis of lymphocytes induced by HDAC inhibitors, nor does loss of Bmf impair apoptosis of B220$^+$ splenic B cells in response to cytokine deprivation, dexamethasone treatment, or BCR ligation. Fig. S2 shows that Bmf-deficient mice mount normal immune responses to T cell–dependent and –independent antigens. Fig. S3 demonstrates that apoptosis induced by UV irradiation or loss of attachment is not impaired in *bmf*$^{-/-}$ MEFs. Fig. S4 demonstrates that anoikis in gastrointestinal epithelial cells is not impaired in the absence of *bim* or *bmf*. Fig. S5 shows cell surface expression of CD4 and CD8 antigens in γ irradiation–induced lymphomas found in thymi and spleen from WT, *bmf*$^{-/-}$, and *p53*$^{+/-}$ mice. Fig. S6 shows normal proliferative responses of FACS-sorted Bmf-deficient B cells in response to different mitogens. The online version of this article is available at http://www.jem.org/cgi/content/full/jem.20071658/DC1.

We are grateful to K. Rossi, C. Soratroi, R. Pfeilschifter, and L. Tai for technical assistance, and to M. Bogner for animal husbandry. We thank A. Tzankov for assessment of histology, E. Stanley for helpful advice on gene targeting, A. Steptoe for ES cell manipulations, G. Böck for cell sorting, C. Mayerl for the pan-cytokeratin antibody, P. Lukas for enabling irradiation of mice, and R. Johnstone for SAHA

This work was supported by grants from the National Health and Medical Research Council (Canberra), the Dr. Josef Steiner Cancer Research Foundation (Bern), the Leukemia and Lymphoma Society, the National institutes of Health to A. Strasser, and the Austrian Science Fund Y212-B13 START and the SFB021, as well as the Association for International Cancer Research to AV. V. Labi is currently supported by a young investigator grant from the Tyrolean Science Fund.

The authors have no conflicting financial interests.

Submitted: 6 August 2007
Accepted: 31 January 2008

REFERENCES

1. Strasser, A. 2005. The role of BH3-only proteins in the immune system. *Nat. Rev. Immunol.* 5:189–200.
2. Danial, N.N., and S.J. Korsmeyer. 2004. Cell death: critical control points. *Cell.* 116:205–219.
3. Zong, W.X., T. Lindsten, A.J. Ross, G.R. MacGregor, and C.B. Thompson. 2001. BH3-only proteins that bind pro-survival Bcl-2 family members fail to induce apoptosis in the absence of Bax and Bak. *Genes Dev.* 15:1481–1486.
4. Wei, M.C., W.X. Zong, E.H. Cheng, T. Lindsten, V. Panoutsakopoulou, A.J. Ross, K.A. Roth, G.R. MacGregor, C.B. Thompson, and S.J. Korsmeyer. 2001. Proapoptotic BAX and BAK: a requisite gateway to mitochondrial dysfunction and death. *Science.* 292:727–730.
5. Certo, M., G. Moore Vdel, M. Nishino, G. Wei, S. Korsmeyer, S.A. Armstrong, and A. Letai. 2006. Mitochondria primed by death signals determine cellular addiction to antiapoptotic BCL-2 family members. *Cancer Cell.* 9:351–365.
6. Willis, S.N., J.I. Fletcher, T. Kaufmann, M.F. van Delft, L. Chen, P.E. Czabotar, H. Ierino, E.F. Lee, W.D. Fairlie, P. Bouillet, et al. 2007. Apoptosis initiated when BH3 ligands engage multiple Bcl-2 homologs, not Bax or Bak. *Science.* 315:856–859.
7. Kuwana, T., L. Bouchier-Hayes, J.E. Chipuk, C. Bonzon, B.A. Sullivan, D.R. Green, and D.D. Newmeyer. 2005. BH3 domains of BH3-only proteins differentially regulate Bax-mediated mitochondrial membrane permeabilization both directly and indirectly. *Mol. Cell.* 17:525–535.
8. Chen, L., S.N. Willis, A. Wei, B.J. Smith, J.I. Fletcher, M.G. Hinds, P.M. Colman, C.L. Day, J.M. Adams, and D.C. Huang. 2005. Differential targeting of prosurvival Bcl-2 proteins by their BH3-only ligands allows complementary apoptotic function. *Mol. Cell.* 17:393–403.
9. Bouillet, P., D. Metcalf, D.C.S. Huang, D.M. Tarlinton, T.W.H. Kay, F. Köntgen, J.M. Adams, and A. Strasser. 1999. Proapoptotic Bcl-2 relative Bim required for certain apoptotic responses, leukocyte homeostasis, and to preclude autoimmunity. *Science.* 286:1735–1738.
10. Coultas, L., P. Bouillet, K.L. Loveland, S. Meachem, H. Perlman, J.M. Adams, and A. Strasser. 2005. Concomitant loss of proapoptotic BH3-only Bcl-2 antagonists Bik and Bim arrests spermatogenesis. *EMBO J.* 24:3963–3973.
11. Yin, X.-M., K. Wang, A. Gross, Y. Zhao, S. Zinkel, B. Klocke, K.A. Roth, and S.J. Korsmeyer. 1999. Bid-deficient mice are resistant to Fas-induced hepatocellular apoptosis. *Nature.* 400:886–891.
12. Kaufmann, T., L. Tai, P.G. Ekert, D.C. Huang, F. Norris, R.K. Lindemann, R.W. Johnstone, V.M. Dixit, and A. Strasser. 2007. The BH3-only protein bid is dispensable for DNA damage- and replicative stress-induced apoptosis or cell-cycle arrest. *Cell.* 129:423–433.
13. Villunger, A., E.M. Michalak, L. Coultas, F. Mullauer, G. Bock, M.J. Ausserlechner, J.M. Adams, and A. Strasser. 2003. p53- and drug-induced apoptotic responses mediated by BH3-only proteins puma and noxa. *Science.* 302:1036–1038.

14. Jeffers, J.R., E. Parganas, Y. Lee, C. Yang, J. Wang, J. Brennan, K.H. MacLean, J. Han, T. Chittenden, J.N. Ihle, et al. 2003. Puma is an essential mediator of p53-dependent and -independent apoptotic pathways. *Cancer Cell.* 4:321–328.
15. You, H., M. Pellegrini, K. Tsuchihara, K. Yamamoto, G. Hacker, M. Erlacher, A. Villunger, and T.W. Mak. 2006. FOXO3a-dependent regulation of Puma in response to cytokine/growth factor withdrawal. *J. Exp. Med.* 203:1657–1663.
16. Erlacher, M., V. Labi, C. Manzl, G. Bock, A. Tzankov, G. Hacker, E. Michalak, A. Strasser, and A. Villunger. 2006. Puma cooperates with Bim, the rate-limiting BH3-only protein in cell death during lymphocyte development, in apoptosis induction. *J. Exp. Med.* 203:2939–2951.
17. Bouillet, P., J.F. Purton, D.I. Godfrey, L.-C. Zhang, L. Coultas, H. Puthalakath, M. Pellegrini, S. Cory, J.M. Adams, and A. Strasser. 2002. BH3-only Bcl-2 family member Bim is required for apoptosis of autoreactive thymocytes. *Nature.* 415:922–926.
18. Villunger, A., V.S. Marsden, Y. Zhan, M. Erlacher, A.M. Lew, P. Bouillet, S. Berzins, D.I. Godfrey, W.R. Heath, and A. Strasser. 2004. Negative selection of semimature CD4+8-HSA+ thymocytes requires the BH3-only protein Bim but is independent of death receptor signaling. *Proc. Natl. Acad. Sci. USA.* 101:7052–7057.
19. Enders, A., P. Bouillet, H. Puthalakath, Y. Xu, D.M. Tarlinton, and A. Strasser. 2003. Loss of the pro-apoptotic BH3-only Bcl-2 family member Bim inhibits BCR stimulation-induced apoptosis and deletion of autoreactive B cells. *J. Exp. Med.* 198:1119–1126.
20. Hildeman, D.A., Y. Zhu, T.C. Mitchell, P. Bouillet, A. Strasser, J. Kappler, and P. Marrack. 2002. Activated T cell death in vivo mediated by pro-apoptotic Bcl-2 family member, Bim. *Immunity.* 16:759–767.
21. Pellegrini, M., G. Belz, P. Bouillet, and A. Strasser. 2003. Shutdown of an acute T cell immune response to viral infection is mediated by the pro-apoptotic Bcl-2 homology 3-only protein Bim. *Proc. Natl. Acad. Sci. USA.* 100:14175–14180.
22. Puthalakath, H., D.C.S. Huang, L.A. O'Reilly, S.M. King, and A. Strasser. 1999. The pro-apoptotic activity of the Bcl-2 family member Bim is regulated by interaction with the dynein motor complex. *Mol. Cell.* 3:287–296.
23. Puthalakath, H., A. Villunger, L.A. O'Reilly, J.G. Beaumont, L. Coultas, R.E. Cheney, D.C.S. Huang, and A. Strasser. 2001. Bmf: a pro-apoptotic BH3-only protein regulated by interaction with the myosin V actin motor complex, activated by anoikis. *Science.* 293:1829–1832.
24. Zhang, Y., M. Adachi, R. Kawamura, and K. Imai. 2006. Bmf is a possible mediator in histone deacetylase inhibitors FK228 and CBHA-induced apoptosis. *Cell Death Differ.* 13:129–140.
25. Wick, W., I. Petersen, R.K. Schmutzler, B. Wolfarth, D. Lenartz, E. Bierhoff, J. Hummerich, D.J. Muller, A.P. Stangl, J. Schramm, et al. 1996. Evidence for a novel tumor suppressor gene on chromosome 15 associated with progression to a metastatic stage in breast cancer. *Oncogene.* 12:973–978.
26. Schmutte, C., G. Tombline, K. Rhiem, M.M. Sadoff, R. Schmutzler, A. von Deimling, and R. Fishel. 1999. Characterization of the human Rad51 genomic locus and examination of tumors with 15q14-15 loss of heterozygosity (LOH). *Cancer Res.* 59:4564–4569.
27. Morales, A.A., A. Olsson, F. Celsing, A. Osterborg, M. Jondal, and L.M. Osorio. 2004. Expression and transcriptional regulation of functionally distinct Bmf isoforms in B-chronic lymphocytic leukemia cells. *Leukemia.* 18:41–47.
28. Ploner, C., J. Rainer, H. Niederegger, M. Eduardoff, A. Villunger, S. Geley, and R. Kofler. 2007. The BCL2 rheostat in glucocorticoid-induced apoptosis of acute lymphoblastic leukemia. *Leukemia.* DOI:10.1038/sj.leu.2405039.
29. Strasser, A., A.W. Harris, D.C.S. Huang, P.H. Krammer, and S. Cory. 1995. Bcl-2 and Fas/APO-1 regulate distinct pathways to lymphocyte apoptosis. *EMBO J.* 14:6136–6147.
30. Erlacher, M., E.M. Michalak, P.N. Kelly, V. Labi, H. Niederegger, L. Coultas, J.M. Adams, A. Strasser, and A. Villunger. 2005. BH3-only proteins Puma and Bim are rate-limiting for {gamma} -radiation and glucocorticoid-induced apoptosis of lymphoid cells in vivo. *Blood.* 106: 4131–4138.
31. Loder, F., B. Mutschler, R.J. Ray, C.J. Paige, P. Sideras, R. Torres, M.C. Lamers, and R. Carsetti. 1999. B cell development in the spleen takes place in discrete steps and is determined by the quality of B cell receptor-derived signals. *J. Exp. Med.* 190:75–89.
32. Frisch, S.M., and R.A. Screaton. 2001. Anoikis mechanisms. *Curr. Opin. Cell Biol.* 13:555–562.
33. Coultas, L., P. Bouillet, E.G. Stanley, T.C. Brodnicki, J.M. Adams, and A. Strasser. 2004. Proapoptotic BH3-only Bcl-2 family member Bik/Blk/Nbk is expressed in hemopoietic and endothelial cells but is redundant for their programmed death. *Mol. Cell. Biol.* 24:1570–1581.
34. Pellegrini, M., P. Bouillet, M. Robati, G.T. Belz, G.M. Davey, and A. Strasser. 2004. Loss of Bim increases T cell production and function in interleukin 7 receptor-deficient mice. *J. Exp. Med.* 200:1189–1195.
35. Oliver, P.M., M. Wang, Y. Zhu, J. White, J. Kappler, and P. Marrack. 2004. Loss of Bim allows precursor B cell survival but not precursor B cell differentiation in the absence of interleukin 7. *J. Exp. Med.* 200:1179–1187.
36. Bouillet, P., S. Cory, L.-C. Zhang, A. Strasser, and J.M. Adams. 2001. Degenerative disorders caused by Bcl-2 deficiency are prevented by loss of its BH3-only antagonist Bim. *Dev. Cell.* 1:645–653.
37. Inoue, S., J. Riley, T.W. Gant, M.J. Dyer, and G.M. Cohen. 2007. Apoptosis induced by histone deacetylase inhibitors in leukemic cells is mediated by Bim and Noxa. *Leukemia.* 21:1773–1782.
38. Shibue, T., K. Takeda, E. Oda, H. Tanaka, H. Murasawa, A. Takaoka, Y. Morishita, S. Akira, T. Taniguchi, and N. Tanaka. 2003. Integral role of Noxa in p53-mediated apoptotic response. *Genes Dev.* 17:2233–2238.
39. Naik, E., E.M. Michalak, A. Villunger, J.M. Adams, and A. Strasser. 2007. Ultraviolet radiation triggers apoptosis of fibroblasts and skin keratinocytes mainly via the BH3-only protein Noxa. *J. Cell Biol.* 176:415–424.
40. Rosen, K., J. Rak, T. Leung, N.M. Dean, R.S. Kerbel, and J. Filmus. 2000. Activated Ras prevents downregulation of Bcl-X(L) triggered by detachment from the extracellular matrix. A mechanism of Ras-induced resistance to anoikis in intestinal epithelial cells. *J. Cell Biol.* 149: 447–456.
41. Rosen, K., J. Rak, J. Jin, R.S. Kerbel, M.J. Newman, and J. Filmus. 1998. Downregulation of the pro-apoptotic protein Bak is required for the ras-induced transformation of intestinal epithelial cells. *Curr. Biol.* 8:1331–1334.
42. Marani, M., D. Hancock, R. Lopes, T. Tenev, J. Downward, and N.R. Lemoine. 2004. Role of Bim in the survival pathway induced by Raf in epithelial cells. *Oncogene.* 23:2431–2441.
43. Fukazawa, H., K. Noguchi, A. Masumi, Y. Murakami, and Y. Uehara. 2004. BimEL is an important determinant for induction of anoikis sensitivity by mitogen-activated protein/extracellular signal-regulated kinase kinase inhibitors. *Mol. Cancer Ther.* 3:1281–1288.
44. Reginato, M.J., K.R. Mills, J.K. Paulus, D.K. Lynch, D.C. Sgroi, J. Debnath, S.K. Muthuswamy, and J.S. Brugge. 2003. Integrins and EGFR coordinately regulate the pro-apoptotic protein Bim to prevent anoikis. *Nat. Cell Biol.* 5:733–740.
45. Wang, P., A.P. Gilmore, and C.H. Streuli. 2004. Bim is an apoptosis sensor that responds to loss of survival signals delivered by epidermal growth factor but not those provided by integrins. *J. Biol. Chem.* 279:41280–41285.
46. Schmelzle, T., A.A. Mailleux, M. Overholtzer, J.S. Carroll, N.L. Solimini, E.S. Lightcap, O.P. Veiby, and J.S. Brugge. 2007. Functional role and oncogene-regulated expression of the BH3-only factor Bmf in mammary epithelial anoikis and morphogenesis. *Proc. Natl. Acad. Sci. USA.* 104:3787–3792.
47. Villunger, A., D.C.S. Huang, N. Holler, J. Tschopp, and A. Strasser. 2000. Fas ligand-induced c-Jun kinase activation in lymphoid cells requires extensive receptor aggregation but is independent of DAXX, and Fas-mediated cell death does not involve DAXX, RIP or RAIDD. *J. Immunol.* 165:1337–1343.